Compartmentalization of Cerebral Cortical Germinal Zones in a Lissencephalic Primate and Gyrencephalic Rodent

Fernando García-Moreno[1], Navneet A. Vasistha[1], Nonata Trevia[1], James A. Bourne[2] and Zoltán Molnár[1]

[1]Department of Physiology, Anatomy and Genetics, University of Oxford, Oxford OX1 3QX, UK and [2]Australian Regenerative Medicine Institute, Monash University, Victoria 3800, Australia

Fernando García-Moreno and Navneet A. Vasistha have contributed equally to this study

Address correspondence to email: zoltan.molnar@dpag.ox.ac.uk.

Previous studies of macaque and human cortices identified cytoarchitectonically distinct germinal zones; the ventricular zone, inner subventricular zone (ISVZ), and outer subventricular zone (OSVZ). To date, the OSVZ has only been described in gyrencephalic brains, separated from the ISVZ by an inner fiber layer and considered a milestone that triggered increased neocortical neurogenesis. However, this observation has only been assessed in a handful of species without the identification of the different progenitor populations. We examined the Amazonian rodent agouti (*Dasyprocta agouti*) and the marmoset monkey (*Callithrix jacchus*) to further understand relationships among progenitor compartmentalization, proportions of various cortical progenitors, and degree of cortical folding. We identified a similar cytoarchitectonic distinction between the OSVZ and ISVZ at midgestation in both species. In the marmoset, we quantified the ventricular and abventricular divisions and observed similar proportions as previously described for the human and ferret brains. The proportions of radial glia, intermediate progenitors, and outer radial glial cell (oRG) populations were similar in midgestation lissencephalic marmoset as in gyrencephalic human or ferret. Our findings suggest that cytoarchitectonic subdivisions of SVZ are an evolutionary trend and not a primate specific feature, and a large population of oRG can be seen regardless of cortical folding.

Keywords: agouti, cortical folding, intermediate progenitors, marmoset, subventricular zone

Introduction

The evolutionary expansion of the cerebral cortex has been correlated with substantial changes in the proliferative compartments of the telencephalon (Rakic 2003; Martínez-Cerdeño et al. 2006). For example, progenitors in the telencephalon of reptiles only divide in the ventricular zone (VZ), while birds present a well-developed secondary germinal compartment, the subventricular zone (SVZ) in the subpallium, and to a lesser extent in the dorsal cortex (Cheung et al. 2007; Striedter and Charvet 2009). In mammals, an innovative dorsal SVZ has evolved, likely related to the increased cortical thickness (Cheung et al. 2007), while in the adult neocortex of the noneutherian mammal, the marsupial (*Monodelphis domestica*), considerably less neurons exist in an arbitrary unit column of their cortex than mouse (Cheung et al. 2010). Nevertheless, during their early postnatal development, their SVZ reveals a similar gene expression pattern (Cheung et al. 2010; Puzzolo and Mallamaci 2010), and there is an abventricular secondary layer of mitotic progenitors that appears relatively late and are considered neurogenic (Cheung et al. 2010) or gliogenic (Puzzolo and Mallamaci 2010). These findings suggest that although the proportions can vary greatly, all species across the mammalian lineage, including marsupials, have a SVZ during cortical development, the appearance of which has been accompanied by the creation of 2 different types of progenitor. First, the intermediate progenitor cells (IPCs) which posses a multipolar cellular body but are not connected to neuroepithelial surfaces and express specific markers including Tbr2 (Kowalczyk et al. 2009). The IPCs, also have the capacity to undergo 1 or 2 subsequent symmetric divisions to amplify the number of neurons (Haubensak et al. 2004; Miyata et al. 2004; Noctor et al. 2004; Noctor et al. 2008). Second, the recently described outer radial glial cells (oRGs), a bipolar progenitor that express Sox2, Pax6, and pVim and posses a basal process extending to the pia (Fietz et al. 2010; Hansen et al. 2010; Reillo et al. 2011; Shitamukai et al. 2011; Wang et al. 2011). oRGs have been described to reside at the upper boundary of the SVZ, specifically the intermediate zone (IZ) of mice but the outer SVZ (OSVZ) of larger brains, hence indicating a separate location for these progenitors. The VZ, ISVZ, and OSVZ can be clearly discerned based on differences in the cytoarchitecture (Smart et al. 2002). The OSVZ lies separated from the ISVZ by an inner fiber layer (IFL). However, the cytoarchitectonic distinctions between these zones have only been described in gyrencephalic brains. Thus, the compartmentalization of SVZ is considered a milestone in triggering cortical neurogenesis to a new evolutionary step (Smart et al. 2002; Dehay and Kennedy, 2007).

Intermediate radial glia or oRG progenitors have been recently identified in the developing mouse cortex (Shitamukai et al. 2011; Wang et al. 2011). While the oRG population reaches 50% of all progenitor cells in human or ferret (Fietz et al. 2010; Hansen et al. 2010; Reillo et al. 2011), they are estimated to be below 10% in mouse (Shitamukai et al. 2011, Wang et al. 2011). Hence some studies suggest a correlation between the enlarged oRG progenitor populations and gyrencephaly (Fietz et al. 2010; Reillo et al. 2011).

We demonstrate here that the gyrencephalic Amazonian rodent, agouti and a lissencephalic nonhuman primate marmoset monkey both possess oRGs from around midgestation and a well organized and cytoarchitectonically distinct OSVZ during neocortical neurogenesis. Moreover, the presence of different subventricular progenitors is not associated with specific germinal layers as pVim positive oRGs, and Tbr2 positive IPCs are present both in ISVZ and in OSVZ but in different proportions. Interestingly, these proportions are not different from the observations made in gyrencephalic brains. We therefore, propose that the association of these discerning cytoarchitectonic features and increased oRG populations with gyrencephaly requires reevaluation.

Materials and Methods

Animals

We examined embryos and neonates of the New World marmoset monkey (*Callithrix jacchus*) at different developmental stages (3 brains at E60, 2 each at E88 and E110; see Fig. 1; gestational period = 145 days). All experiments were conducted in accordance with the Australian Code of Practice for the Care and Use of Animals for Scientific Purposes and were approved by the Monash University Animal Ethics Committee, which also monitored the welfare of the animals. Individuals were overdosed with the anesthetic pentobarbitone sodium (100 mg kg^{-1}) and transcardially perfused with 0.1 M heparinized phosphate buffer (PB; pH 7.2) followed by 4% paraformaldehyde in 0.1 M PB. Cerebral tissues were immediately removed and postfixed for 24 h in 4% paraformaldehyde in 0.1 M PB containing 10% sucrose. Cryoprotection was achieved by serially transferring the tissue through solutions of 20% and 30% sucrose in 0.1 M PB before being frozen in OCT (Sakura Finetek) embedding compound. Coronal frozen sections of the hemispheres (20-25 μm) were cut on a cryostat (Leica) and mounted on superfrost glass slides (VWR International).

Dasyprocta agouti were obtained from the Museum Emilio Goeldi (Belem, Para, Brazil) and kept at Biological Institute of Federal University of Para. All animals were handled in accordance with "Principles of Laboratory Animal Care" National Institutes of Health [NIH]. Timed pregnant dams were anesthetized with a solution of ketamine (100 g kg^{-1}) and xylazine (10 mg kg^{-1}) (Konig Laboratories) and transcardially perfused with heparinized saline (5000 U/L) followed by 4% paraformaldehyde in 0.1 M PB, pH 7.2-7.4. E52 embryos (gestational period lasts approximately 110 days) were removed and the brains fixed by immersion in 4% paraformaldehyde at 4 °C, cryoprotected with 30% sucrose overnight, and then frozen in OCT compound. Sections were cut at 40 μm on a cryostat (Leica), air dried, and stored at −20 °C.

Immunohistochemistry

Immunohistochemistry was performed as previously described (Hoerder-Suabedissen et al. 2009) using the following primary antibodies: mouse anti-phospho vimentin (pVim; MBL; 1/200); mouse anti-phospho histone H3 (pH3; Abcam; 1/1000); rabbit anti-pH3 (Abcam; 1/500); rabbit anti-Tbr2 (gift from Prof Robert Hevner, University of Washington, Seattle; 1/2000); rabbit anti-Sox2 (Abcam; 1/1000); rabbit anti-Ki67 (Abcam; 1/500); mouse anti-Snap25 (Covance; 1/500), and mouse anti-srGAP1 (Abcam; 1/100). Primary antibodies were diluted in phosphate buffered saline containing 0.1% Triton X-100 (BDH, London, UK) and 1% Goat or Donkey Serum (Sigma, UK). Sections were incubated overnight at 4 °C. After several rinses, sections were subsequently incubated with fluorescent secondary antibodies diluted in the same solution as for the primary antibodies. Alexa Fluor conjugated secondary antibodies (Invitrogen, 1/500) were used for fluorescent detection. DAPI (4′,6-diamidino-2-phenylindole; Invitrogen) and Nissl substance (cresyl violet) used for counterstaining tissues (Warner et al., 2010).

Sections were first viewed under a fluorescent microscope (Leica DMR, Leica) and selected for confocal imaging. Confocal images were taken on a LSM710 confocal microscope (Carl Zeiss Microimaging). Basal processes of suspected oRG cells (see examples in Figs. 3E and 4G) were confirmed by capturing Z-stacks using the ZEN software (Carl Zeiss).

All images were converted to TIFF format for postprocessing with Adobe CS3 (Adobe Inc.). Image analysis was performed using ImageJ (NIH) software.

Plane of division measurements were taken from sections stained with pH3 on single confocal stacks using the angle tool in ImageJ. All measurements were done parallel to the ventricular surface while all angles were calculated between 0 and 90°. Furthermore, in all cell counts, the number of cells counted is represented by *n* value within parentheses.

Results

The agouti is generally considered a gyrencephalic rodent and the marmoset a lissencephalic nonhuman primate. In terms of gyrification indices (GI), the agouti has a GI of 1.23 (Pillay and Manger 2007) while the marmoset varies slightly with a GI of 1.2 (Rogers et al. 2010). This is in contrast to brains of more convoluted species such as ferret, GI of 1.8 (Neal et al. 2007) and humans with a GI of 2.99 (Pillay and Manger 2007). However, the marmoset brain is strictly speaking not entirely smooth and neither is the agouti clearly gyrencephalic. The adult agouti possesses large sulci extending parallel to the midsagittal position and another at the ventrolateral aspect of the brain. These sulci are already apparent at midgestation (Fig. 1B), although some further maturation occurs subsequently (Fig. 1B,G). The developing marmoset brain is lissencephalic, and it remains largely so until birth, with only the calcarine sulcus evident on the medial surface (Fig. 1H, P1 panels). In the adult marmoset, a prominent lateral sulcus is apparent (Fig. 1L), however, a large proportion of the convexity of the marmoset telencephalic vesicle shows no obvious sulci or gyri until birth (Fig. 1).

In order to study the similarities and differences in their cortical architecture, we studied coronal sections of embryonic brains of both species using Nissl substance and DAPI. In addition, we employed pH3 immunostaining to examine the sites of progenitor division. On Nissl substance and DAPI counterstained coronal sections of the E52 agouti and E88 marmoset parietal cortex, the compartmentalization of the germinal zone is clearly apparent (Fig. 1C,D and Fig. 1I,J, respectively). pH3 immunostaining revealed ventricular and abventricular mitotic profiles in both species.

Acetyl choline-esterase activity and Snap25 immunoreactivity have both been associated with early telencephalic fiber systems, including the periventricular fibers in the cortical germinal zone (Ulfig et al. 2000; Smart et al. 2002; Vasung et al. 2011). We utilized Snap25 immunohistochemistry in combination with pH3 and DAPI counterstaining to further characterize the position of the IFL in relation to the mitotic profiles and the cytoarchitecture of the cortical germinal zones of the marmoset. Snap25 expression revealed a broad band of fiber fascicles extending through the internal capsule (below the ganglionic eminence close to the anlage of the basal ganglia) toward the IZ of the dorsal cortex (Fig. 2A). The pH3 immunoreactive mitotic profiles were abundant both in the VZ and in the SVZs. At E60, the IZ and SVZ contained dense Snap25 immunoreactive fibers, but the VZ and the cortical plate (CP) showed no or very little fiber labeling (Fig. 2B). By E88, a fiber bundle, the IFL became apparent between the ISVZ and OSVZ. All of these layers contained numerous pH3 immunoreactive mitotic profiles (Fig. 2C,D). With the exception of the lower part of the OSVZ, the Snap25 immunoreactive fibers extended with parallel trajectories to the pial and ventricular surfaces. The ventral part of the OSVZ contained fibers with perpendicular trajectories to the ventricular surface (Fig. 2D). These observations further demonstrate that marmoset cortical germinal zone is compartmentalized in a very similar manner as previously described for macaque and human (Smart et al. 2002; Vasung et al. 2011).

Having demonstrated similar cytoarchitectonic arrangement in the germinal compartments of agouti and marmoset embryonic brains, we then focused on marmoset neocortical development at 2 earlier stages (E60 and E88) in order to study the distribution and proportions of the several subventricular progenitor subtypes. Marmoset embryos aged E60 do not present any sulci or gyri at the telencephalic surface (Fig. 3A). Cortical layering (complete by E130) at this early stage of neurogenesis revealed a densely packed VZ, a loosely packed
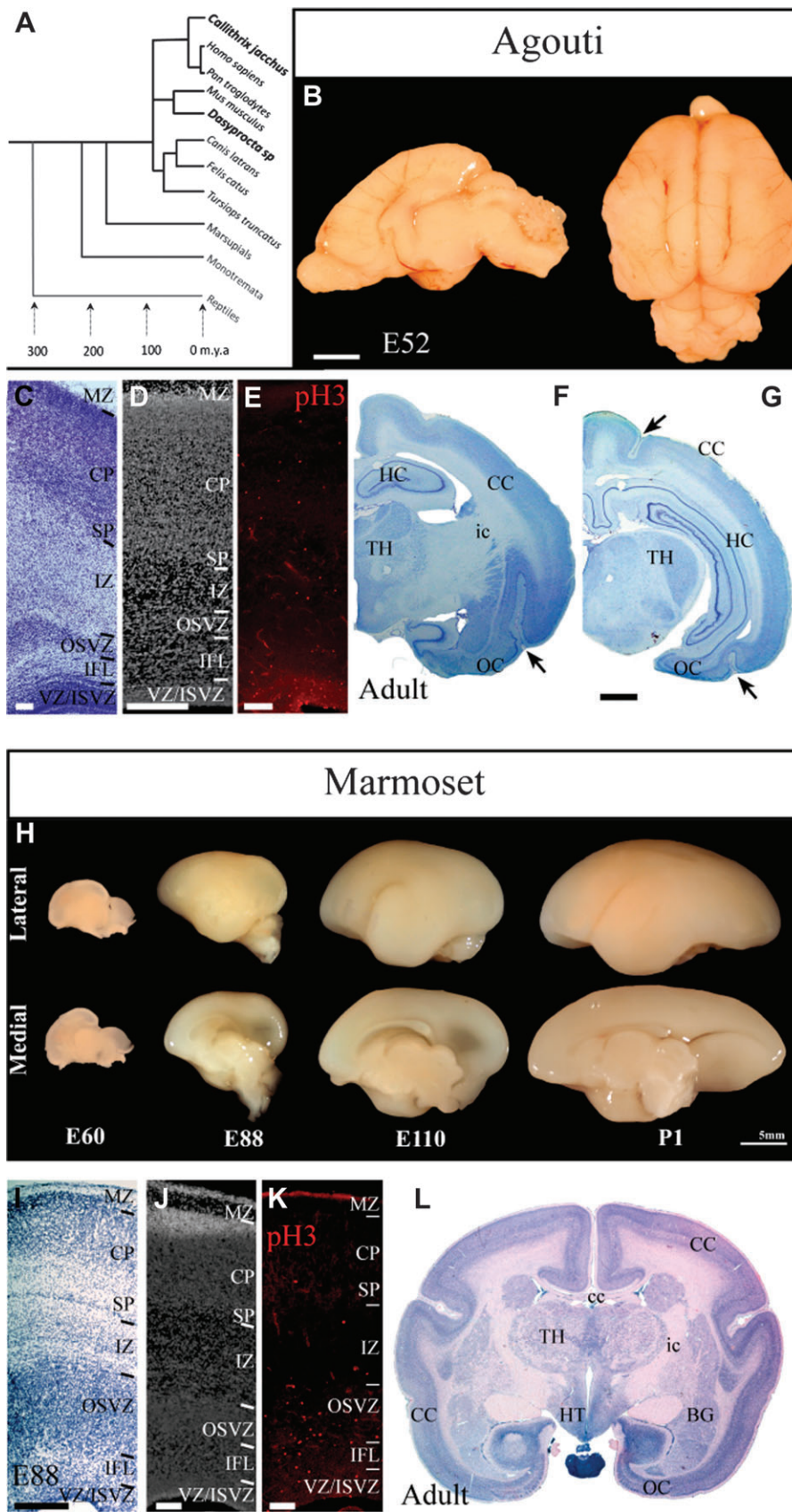
Figure 1. Comparative neuroanatomy of the developing and adult brains of agouti (*B–F*) and marmoset (*G–J*). (*A*) Schematic phylogenetic tree showing the evolutionary relationship between both mammalian species into the Rodentia and Primate Orders, respectively. (*B*) Medial and dorsal views of agouti brains at E52 developmental stage. Rostral is at the left and the top, respectively. (*C*) Nissl staining, (*D*) DAPI labeling, and (*E*) pH3 immunostaining of the developmental cerebral cortex showing the

zone at the SVZ, and the incipient origins of the fiber rich IZ and the CP with the marginal zone lying most superficially below the pial surface. Furthermore, molecular characterization of the various progenitors at E60 revealed no obvious distinctions within the SVZ at this stage (Fig. 3). Ki67 staining was observed in both the VZ and the SVZ representing the germinal zones at this age (Fig. 3C). In the SVZ, Ki67 demonstrated a dispersed expression with few immunoreactive cells located at the outer margins. As with Ki67, pH3 immunoreactive (pH3+) cells were observed mostly in the VZ and SVZ (Fig. 3D). To identify the recently described oRG cells,
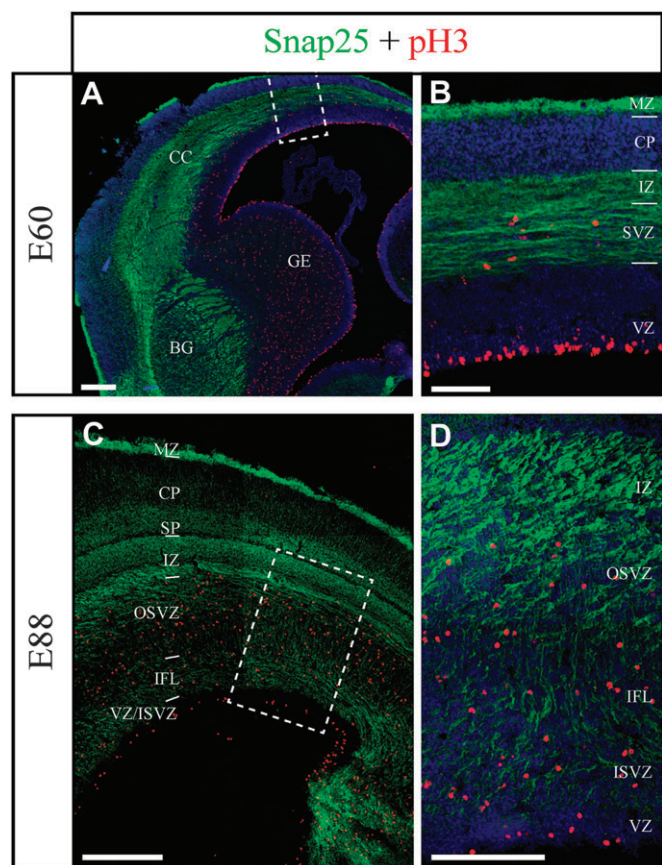
we employed phospho-vimentin (pVim) immunostaining (Fig. 3E). pVim expression followed a pattern very similar to pH3 on account of both being mitotic cell markers (Fig. 3E inset; Kamei et al. 1998; Weissman et al. 2003). pH3 expression is observed prior to the beginning of mitotic prophase and thus precedes the expression of pVim. Additionally, pH3 expression diminishes toward the beginning of telophase, while pVim expression can still be seen at the point of cytokinesis. Colocalization studies of these 2 markers revealed 61% of pH3 cells in the dorsal forebrain express pVim (Weissman et al. 2003).

To probe the identity of oRG cells in marmoset, we immunostained for both Sox2 and pVim (Fig. 3F,H–J). We defined the oRG as cells expressing both Sox2 and pVim and with a visible pially directed basal process. Sox2 expression at E60 was mostly confined to the VZ with a few labeled cells in the SVZ. In the VZ ($n = 109$), 87.2% (±7.9 Standard Error of Difference of Means [SED], $P < 0.005$, $n = 95$) of pH3+ cells were also Sox2 immunoreactive. Interestingly, already by E60, 16.19% of all Sox2+ cells were located in the SVZ demonstrating a heterogeneity in the progenitor population at this age. Of the pVim+ cells studied in the SVZ ($n = 47$), 40.4% (±23.6 SED, $P < 0.005$, $n = 19$) colabeled for Sox2 demonstrating that a significant population of Sox2+ cells divided away from the VZ. This population represents the recently discovered oRG cells. oRG cells have been demonstrated to express both Sox2 and Pax6, while being negative for the IPC marker Tbr2 (Fietz et al. 2010; Hansen et al. 2010; Reillo et al. 2011; Shitamukai et al. 2011; Wang et al. 2011). Consistent with these findings, we found oRG cells double labeled for Sox2 and pVim at the outer border of the SVZ (Fig. 3I,J). The absence of Sox2 staining in nearly 60% of the pVim+ cells with basal processes in the SVZ (data not shown) suggests either a genetic heterogeneity or a transcriptional repression.

In addition to staining for RG and oRG progenitors, we also performed Tbr2 immunostaining to study IPCs in the developing neocortex (Fig. 3G,H,K,L). We noted that Tbr2 immunoreactivity was restricted largely to the SVZ with a few cells also labeled in the VZ and IZ. This further represents that at E60, the VZ and SVZ are the only major germinal zones in the marmoset. To study the proportion of dividing IPCs, we double stained for Tbr2/pH3 (Fig. 3K,L). Of all pH3+ cells observed, no colabeling was observed with Tbr2 in the VZ ($n = 92$), while 86.2% (±10.9 SED, $P < 0.05$ $n = 92$) of pH3+ cells in the SVZ colabeled for Tbr2.

We also measured the plane of division of pH3+ cells in the VZ and SVZ ($n = 111$ cells across 3 brains) and found that at E60 divisions at the ventricular epithelium was largely either perpendicular (60–90°, $n = 28$) or horizontal (0–30°, $n = 32$) with reference to the ventricular surface (Fig. 3M). In the SVZ, divisions were either horizontal ($n = 12$) or oblique ($n = 13$) with few cells dividing perpendicular to the ventricular surface ($n = 7$).

Having found Sox2+ oRGs and Tbr2 immunoreactive IPCs at E60, we conclude that the appearance of these progenitors preceded the split of the SVZ into inner and outer zones.

Figure 2. Cytoarchitecture and fiber staining with DAPI and for Snap25 immunoreactivity. Snap25 immunoreactivity revealed and extensive fiber layer in germinal zones in E60 (A,B) and E88 (C,D) marmoset neocortex. Coronal sections through the forebrain, including parietal cortex, was stained with DAPI (blue), for Snap25 (green), and pH3 (red) immunoreactivity. (A) At E60 Snap25 immunoreactivity revealed a broad band of fiber fascicles crossing below the ganglionic eminence (GE) close to the anlage of the basal ganglia (BG). A thick band of Snap25 immunoreactive fibers extended dorsally in the IZ of the cortex (CC). (B) The SVZ contained pH3 immunoreactive nuclei. The VZ and the CP showed relatively less fiber labeling at this stage. (C) At E88 the Snap25 immunoreactive fibers showed variations in their density and orientation in different layers. Subplate (SP), upper part of OSVZ, and internal fiber layer (IFL) contained fibers with parallel trajectories to the pial and ventricular surfaces. The fibers were perpendicular to the ventricular surface with the lower part of the OSVZ. The VZ contained relatively little labeled fibers. Scale bars: 200 μm for all.

compartmentalization of the proliferative domains. (F) and (G) Nissl staining of the forebrain in coronal sections. Black arrows indicate the presence of 2 mayor gyri at the cerebral cortex. (H) Lateral (top row) and medial (bottom row) views of marmoset brains at various stages of embryonic development and first postnatal day. Notice the smooth cortical surface and the remarkable growth of the occipital lobe (right). Dorsal is at the top. (I) Nissl staining, (J) DAPI labeling, and (K) pH3 immunostaining of the developmental cerebral cortex at E88 illustrating the compartmentalization of the proliferative domains. (L) Nissl substance staining of the entire adult marmoset forebrain in a coronal section. BG: basal ganglia; CC: cerebral cortex; cc: corpus callosum; ic: internal capsule; HC: hippocampus; HT: hypothalamus; MZ: marginal zone; OC: olfactory cortex; TH: thalamus. Scale bars: (B), (F), (G) and (H) 5 mm; (C)–(E) and (I)–(K) 250 μm.
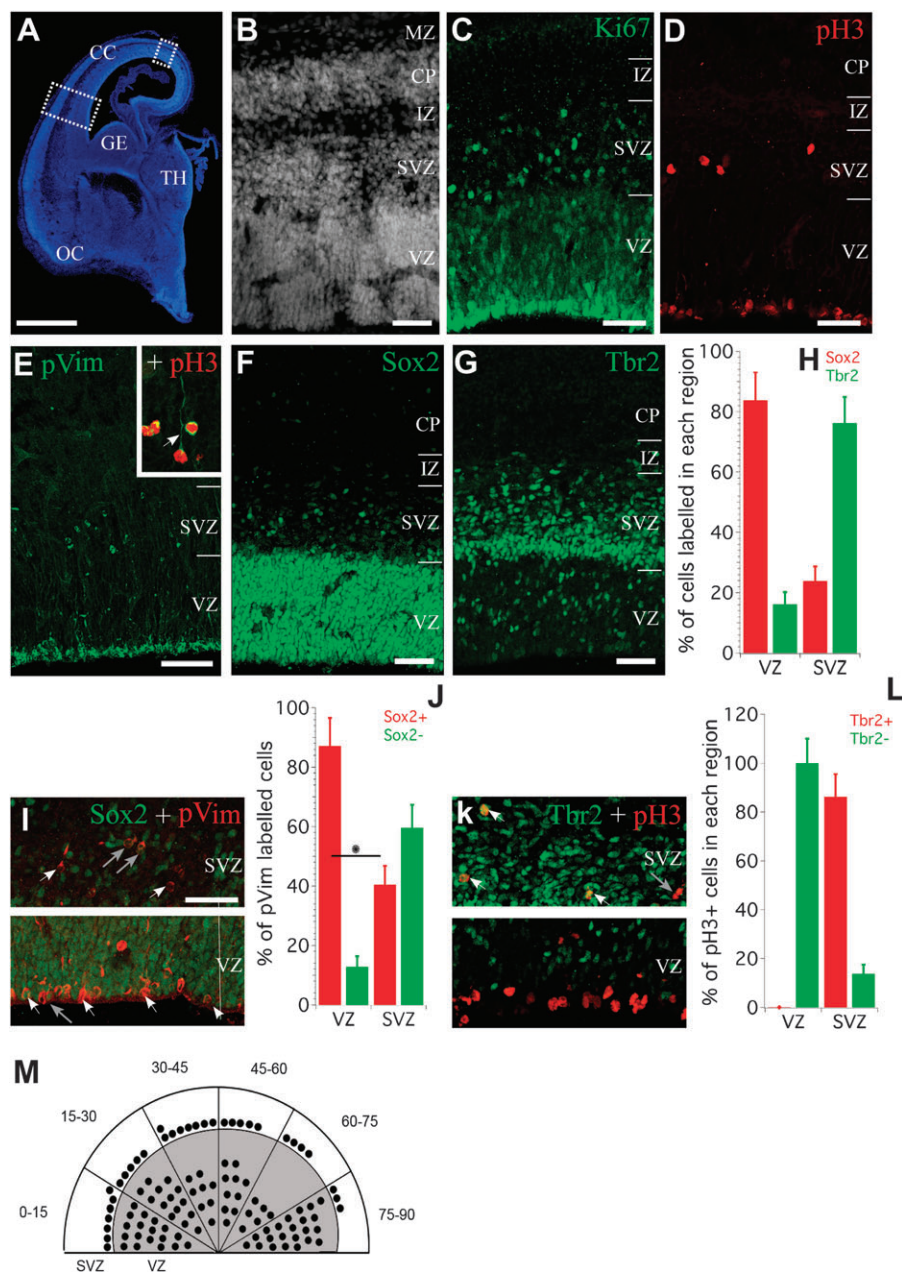
Figure 3. Cytoarchitecture of the proliferative domains in E60 marmoset embryos. Coronal section of the forebrain stained with DAPI. Dashed rectangles indicate the cortical level where the pictures were taken, showing the difference in cortical thickness among lateral and dorsal cortices. (*B*) Cortical layering at early neurogenesis. Ki67 (*C*), pH3 (*D*), and pVim (*E*) immunostaining revealed proliferative domains. The 3 of them presented 2 distinguishable domains of cellular division, a deep one in the surface of VZ and a secondary one in the SVZ. Inset in (*E*) shows the double labeling of SVZ progenitors with pVim and pH3, white arrow points to the basal process of a presumptive oRG. (*F*) Sox2 immunostaining revealed a strong labeling at the VZ, whereas only some not-packed SVZ progenitors expressed it. (*G*) Tbr2 immunostaining showed a majority of immunoreactive cells at the SVZ. (*H*) Graph presenting the percentage of Sox2 and Tbr2 positive cells in each proliferative domain. At E60 Sox2 progenitors were more present at the VZ and Tbr2 progenitors were preferentially found in the SVZ. (*I*) Double labeling with Sox2 (green) and pVim (red) at the SVZ (top) and the VZ (bottom). (*J*) Quantification of pVim progenitors expressing Sox2 at E60. pVim immunoreactive progenitors at the VZ mainly expressed Sox2 (87.2 ± 7.9%). At the SVZ, there were 40.4 ± 23.6% of pVim progenitors expressing Sox2. (*K*) Double labeling with Tbr2 (green) and pH3 (red) at the SVZ (top) and the VZ (bottom). (*L*) Graph presenting the percentage of progenitors expressing Tbr2 in each proliferative domain. Mitotic cells at the VZ were not immunoreactive for Tbr2 (0 cells in 92), whereas 86.2 ± 10.9% of SVZ pH3+ progenitors expressed it. (*M*) Graph shows division planes of mitotic cells in the VZ and SVZ of E60 marmoset. Majority of cells divide either at acute angles (0–30; $n = 32$) or perpendicular to the VZ (60–90, $n = 28$) as compared with the SVZ where the division planes are random. CC: cerebral cortex; GE: ganglionic eminence; MZ: marginal zone; OC: olfactory cortex; TH: thalamus. Asterisks indicate P values (one-tailed Student's t-test). Scale bars: (*A*) 1 mm; (*C*–*G*) and (*I*–*K*) in (K) 50 μm.

Next we studied the specific changes taking place in the developing neocortex at the level of the germinal zone. In the E88 marmoset, initial characterization with Nissl substance and DAPI revealed a subdivision of the SVZ into inner and outer compartments, ISVZ and OSVZ (Figs. 1*I–K* and 3). In contrast to E60, at E88, Ki67 expression was observed in all germinal layers from the VZ to the OSVZ including the IFL (Fig. 4*E*). This was further confirmed by pH3 (Fig. 4*F*) and pVim expression (Fig. 4*G*), indicating that the subdivision of the SVZ takes place during the epoch between E60 and E88, creating an additional sector within the germinal zone.

This compartmentalization is still present at E110 (Fig. 5*A*). Sox2 expression was found in all germinal layers including the IFL (Fig. 4*H,J*). In fact, more Sox2+ cells were seen in the IFL and OSVZ as compared with the VZ, where most of the radial glial population is believed to reside (17.09% VZ; 20.52% ISVZ; 29.16% IFL; and 33.23% OSVZ, respectively, *P* values < 0.05, minimum of 500 cells counted in each zone). Thus, more than half of the Sox2+ population resides outside the confines of the VZ/ISVZ by E88, suggesting that the VZ is no longer the major germinal zone at this stage. Tbr2 expression at E88 was similar to Sox2 except that Tbr2+ cells were absent in the VZ (Fig. 4*I,K*; 0.46% VZ, $n = 11$, $P < 0.05 \times 10^{-4}$). Importantly, while expression in the ISVZ was in the form of a discernible band of cells parallel to the VZ, expression in the other regions was in a more diffuse pattern similar to the Sox2 expression in these regions. With the expression of Tbr2, this was increased in both the OSVZ and the ISVZ (Fig. 4*I*; 43.57% OSVZ, 32.34% ISVZ, $P < 0.005$, minimum of 500 cells counted in each zone except the VZ) compared with Sox2 expression, which was more equitable across the different zones (Fig. 4*K*). Double staining for Tbr2 and pVim labeled cells similar to the pH3 expression profile, however, none of the Tbr2+/pVim+ cells had a basal process (data not shown), further adding to previous observations on the nature of oRGs.

Orientations of metaphasic and anaphasic cell divisions in the VZ were mainly found to be perpendicular ($n = 8$) as compared with horizontal ($n = 5$) with the rest showing an oblique plane (total cells counted = 16). However, the majority of OSVZ divisions were oblique (16/25). Description of division planes in the ISVZ and IFL could not be made due to the small number of pH3+ cells counted across different sections ($n = 10$ and 12, respectively, out of 63).

Cumulatively, this indicates that oRG progenitors in the marmoset are not selectively located in the OSVZ but are also present in the ISVZ, albeit at lower levels. Alternatively, the OSVZ progenitors observed in the ISVZ and IFL could also be ones newly born from the radial glial progenitors and in the process of translocating to their final location in the OSVZ (as suggested by Wang et al. 2011).

In order to further compare the cortical germinal zones between the lissencephalic primate and a gyrencephalic rodent, we examined several key factors involved on compartmentalization of the SVZ and various subtypes of progenitors in embryonic agouti brains. Sox2 and Snap25 immunostaining in E52 agouti cortices revealed a similar expression pattern as that seen in marmoset (Fig. 6*C,D*). Sox2 immunoreactivity was dense in the VZ with a diffuse pattern in the remaining SVZ extending up to the IZ (Fig. 6*C*). This demonstrates that by E52, a large amount of mitosis occurs out of the VZ.

We also used Snap25 and srGAP1 immunostaining to examine the fiber layers. srGAP1 has been recently demonstrated to be expressed in fetal human cortices in the SVZ and later in the neocortical layers (Ip et al. 2011). Additionally, srGAP1 immunoreactivity in the human fetus is strong in the IFL by 12 PCW (postconception week) and more broad in the IFL, IZ, and subplate by 15 PCW (Ip et al. 2011; Molnár and Clowry 2011). In line with this, we observed both Snap25 and srGAP1 immunoreactive fibers in the IFL in the agouti germinal zone (Fig. 6*D,E*). However, compared with Snap25, srGAP1 immunostaining pattern was more diffuse. Taken together, these data demonstrating the cytoarchitecture, the pattern of progenitors, and the fiber distribution all provide evidence of a clear compartmentalization of the SVZ in developing agouti cortex at E52. This also affirms the presence of fibers in the developing germinal zones in species with an expanded SVZ. The anatomical placement of this fiber bundle might indicate its role in regulating the cell cycle, and thus its origin and detailed pattern of interaction will need further investigation. Limitations of tissue availability from other stages and the differences in antibody reactivity in agouti tissue prevented us from studying several other markers in both agouti and marmoset.

Discussion

In this study, we demonstrate that the developmental program for neocortical neurogenesis is largely conserved between representatives of the Rodent and Primate Order, regardless of the extent of gyrification of the neocortex. Both, the marmoset and the agouti SVZ appear compartmentalized due to the presence of IFL fibers and posses a large population of oRGs.

Understanding how an enlarged CP with increasing capacity for establishing new patterns of connectivity is a central issue for developmental and evolutionary neurobiology (Molnár 2011). One of the first models linking cortical expansion during evolution was the founder cell hypothesis (Rakic 1995). According to this model, cortical expansion is the result of changes in proliferation kinetics that increase the number of radial columnar units without changing the number of neurons within each unit significantly. Therefore the detailed study of timing, control, and ratio of symmetric and asymmetric modes of cell divisions in the proliferative zone is of major interest for understanding evolution.

The contribution of the multiple progenitor population toward development of the neocortex is currently not known. There is a self-renewing progenitor cell population, namely the radial progenitors (Malatesta et al. 2000; Noctor et al. 2001; Miyata et al. 2004) that generate a single neuron per division and a basal progenitor pool that amplifies neuronal output by dividing symmetrically to provide 2 neurons (Haubensak et al. 2004; Noctor et al. 2004). Evolution of the neocortex can be achieved by changes to this dual progenitor system. That is to say, increases in the proliferative activity of the progenitors at the behest of cell-cycle parameters (Martínez-Cerdeño et al. 2006; Pilaz et al. 2009) or by an increase in progenitors as noted during evolution between sauropsids and therapsids (Cheung et al. 2007; Striedter and Charvet 2008).

The progenitor pool termed as oRGs (Fietz et al. 2010; Hansen et al. 2010; Reillo et al. 2011) and the transient progenitor pool close to the pallial–subpallial boundary (Teissier et al. 2010) might suggest that the evolution of the neocortex has proceeded by means of additional progenitor subtypes. These progenitor populations are now better defined and pVim, Sox2, and Tbr2 can distinguish populations in the SVZ, however, their contribution towards the development and evolution of the neocortex is yet to be described.

Recently, compartmentalization and diversification of the SVZ has been proposed to be a key step in evolution of cortical neurogenesis, while it has been specifically related to gyrencephalic brains (Fietz et al. 2010; Reillo et al. 2011) as well as nonhuman primates (Smart et al. 2002; Dehay and Kennedy 2007). The cytoarchitectonic distinctions in the germinal zone and the OSVZ were initially described to be primate, including human, specific in the presumptive primary visual cortex (Smart et al. 2002) and later described to contain both Pax6- and Tbr2-expressing progenitor cells, thereby indicating its dual nature (Bayatti et al. 2008). OSVZ progenitors or oRGs (or
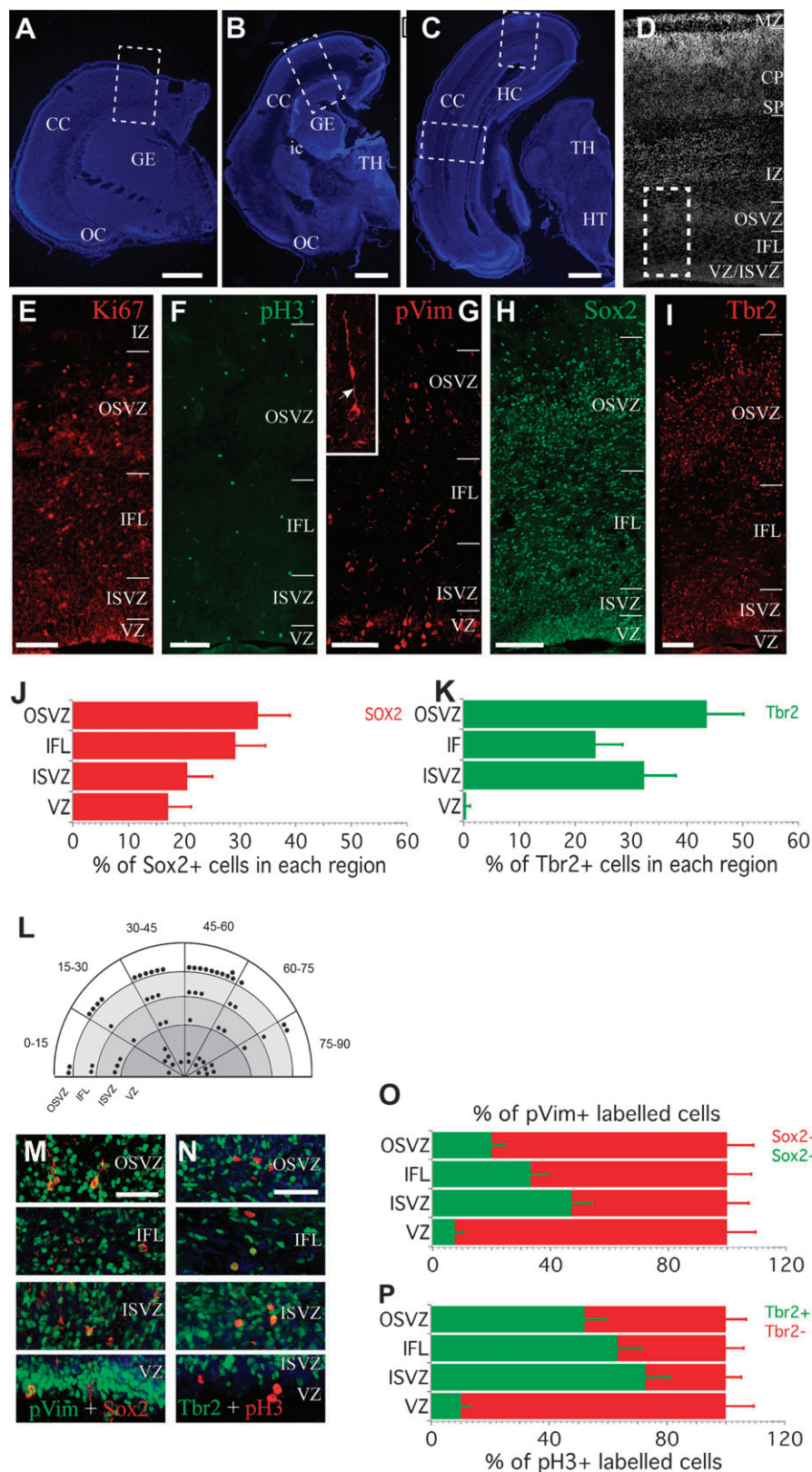
Figure 4. Cytoarchitectonic distinctions between OSVZ and ISVZ of the cortical proliferative domains on E88 marmoset embryos. (A–C) Coronal sections of the forebrain stained with DAPI, from rostral to caudal. Dashed rectangles indicate the cortical level where the pictures were taken. (*D*) Cortical layering at midneurogenesis. Ki67 (*E*), pH3 (*F*), and pVim (*G*) immunostaining revealed proliferative domains. The 3 of them presented 4 distinguishable domains of cellular division, a deep one in the surface VZ and above it a secondary (SVZ) subdivided into superficial (OSVZ) and deeper (ISVZ) layers split by a more prominent fiber layer (IFL). Inset in G shows a presumptive oRG in which basal process is pointed by a white arrow. (*H*) Sox2 immunostaining revealed a strong labeling of densely packed progenitors at the VZ and equally distributed labeling along the different SVZ layers. (*I*) Tbr2 immunostaining presented a majority of immunoreactive cells at the SVZ and only some exception progenitors at the VZ. (*J*) and (*K*) Graphs presenting the percentage of Sox2 and Tbr2 positive cells in each proliferative domain. At E88, Sox2 progenitors were widely distributed along the proliferative domains. On the
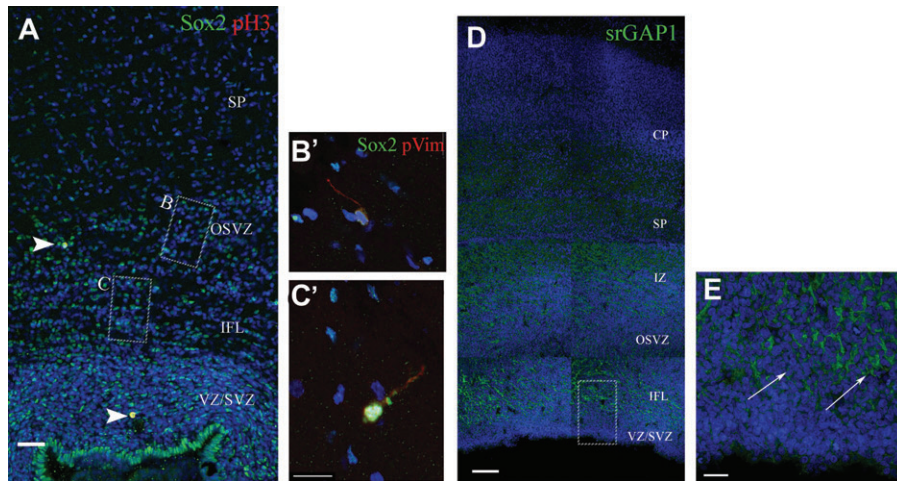
Figure 5. Compartmentalization of cortical germinal zone in the E110 marmoset. (*A*) Double immunostaining for Sox2 (green) and pH3 (red) reveals a similar compartmentalization as seen in E88 cortex with the ISVZ and OSVZ bisected by the ingrowth of a narrow fiber bundle (IFL). Sox2 expression can be seen prominently in the VZ and decreases away from it. Arrowheads indicate the pH3+ cells. Few pH3 cells are seen at this stage indicating end of neurogenesis. Scale bar: 100 μm. (*B′–C′*): Sox2 (green) and pVim (red) double immunoreactive oRG cells taken from the region indicated in (*A*) with a characteristic pVim + basal process. (*B′*) shows an oRG from the OSVZ, the IFL, while C′ shows an oRG in the IFL. Scale bars: (*B′* and *C′*): 50 μm. (*D*) srGAP1 (green) immunostaining to further demonstrate the periventricular fiber layers present in the E88 cortex. Strong srGAP1 immunoreactivity is seen in the IFL and also in the IZ and SP. Together with the Snap25 staining in Figure 4, this demonstrates the presence of fiber layers in the germinal zone of the developing cortex. (*E*) Inset showing high power image taken from the VZ/SVZ area indicated with box in (*D*) further illustrating the srGAP1 immunoreactive fibers in IFL. Arrows indicate fiber fasciculations surrounding progenitor cells. Scale bars (*D*) and (*E*) 100 μm.

intermediate radial glia) have also been demonstrated to be present in the ferret neocortex, a gyrencephalic Canid (Fietz et al. 2010), and more recently in mice (Shitamukai et al. 2011; Wang et al. 2011) but not the cytoarchitectonic distinctions between OSVZ and ISVZ. Our analysis demonstrated that in marmoset the pVim positive oRGs and Tbr2 positive IPCs were not restricted to ISVZ or OSVZ but were present in both but in different proportions.

The examples of agouti and marmoset in this study suggest that the cytoarchitectonic subdivision of the neocortical germinal zone into the OSVZ and ISVZ by the IFL and the presence of the large population of oRG are evolutionary trends in larger brains and not primate or gyrencephalic brain specific features. Instead, the compartmentalization of germinal zones (ISVZ/OSVZ) and a concomitant increase in the oRG and IPC population is a more prudent indicator of the evolutionary mechanism leading to an expansion of the neocortex regardless of the folding pattern of the brain.

In the marmoset, we observed increases in both oRG and IPC populations during development. Since IPCs can amplify the output of neurons, the presence of an increased Tbr2+ population may lead to an increase in the neuronal population and eventually to cortical thickness. Furthermore, lineage studies are required to test the hypothesis that certain intermediate progenitors contribute to particular layers or cell types (Pontious et al. 2008; Kowalczyk et al. 2009; Molnár 2011). Moreover, quantitative analysis of neocortical cell types in different regions in the adult cortex and quantitative assessment of various progenitors in the germinal zone during embryonic development are required by using isometric fractionation in combination with markers of progenitors and neocortical cell types (see methods used by Collins et al. 2010).

There are possible mechanisms how the increase of these populations might stimulate the increased generation and migration of interneurons. Broccoli et al. (Sessa et al. 2010) demonstrated that Tbr2 directs migration of interneurons through chemokine receptors. It is conceivable that an additional Tbr2+ positive germinal zone would attract more interneurons also leading to an increase in neuronal numbers and cortical thickness.

In line with previous studies correlating the presence of an SVZ with a larger neocortex (Striedter and Charvet 2009; Cheung et al. 2010), this raises the possibility that the evolution of the OSVZ with oRG progenitors might be a more potent indicator toward the evolution of a larger brain with faster development irrespective of the order or folding pattern. Since both subtypes of progenitors (IPCs and oRGs) are present in the OSVZ, it indicates that the OSVZ is neither a novelty nor a trigger in terms of cortical evolution but rather it is a proliferative layer similar to the ISVZ, only different in terms of progenitor proportions and location regarding to the IFL.

The relevance of the IFL that separates the ISVZ from the OSVZ is also unknown. However, one hypothesis is that the earliest thalamocortical projections constitute the outer fiber layer while some later ones contribute to the IFL (Lukaszewicz et al. 2005). If some of the fibers in the IFL indeed originate from the thalamus, then species with cytoarchitectonic distinctions between the OSVZ and ISVZ would have thalamic fibers in

other hand, almost all of the Tbr2 cells appeared at the SVZ, with a 77% of cells in the ISVZ/OSVZ. (*L*) Division planes of mitotic cells in the different cortical germinal zones of the E88 marmoset. In the VZ division planes are as at E60: either vertical or perpendicular (*n* = 5 and 8, respectively). However, in the OSVZ, division planes are mostly oblique (30–60, *n* = 16). (*M*) Double labeling with Sox2 (green) and pVim (red) at the 4 proliferative domains. (*N*) Double labeling with Tbr2 (green) and pH3 (red). (*O*) Quantification of pVim progenitors expressing Sox2 at E88. (*P*) Graph presenting the percentage of progenitors expressing Tbr2 in each proliferative domain. CC: cerebral cortex; GE: ganglionic eminence; HT: hypothalamus; MZ: marginal zone; OC: olfactory cortex; SP: subplate; TH: thalamus. Asterisks indicate *P* values (one tailed Student's *t*-test). Scale bars: (*A–C*) 1 mm; (*E–I*), (*M*), and (*O*) 100 μm.
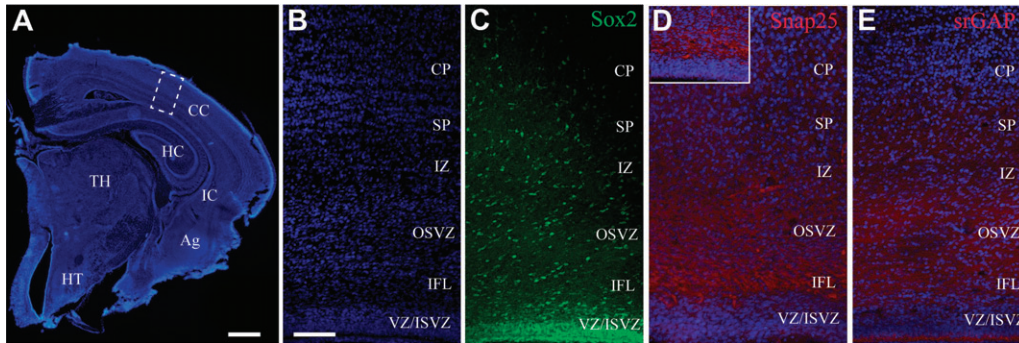
Figure 6. Cytoarchitectonic subdivisions in the E52 agouti cortical germinal zone. (*A*) Low power image of a coronal section of agouti cortex stained with DAPI. Dashed rectangle indicates the cortical region where the higher magnification pictures were taken from. (*B*) Patterning observed in the E52 agouti cortical wall as seen with DAPI staining. A cell dense VZ/SVZ and OSVZ zone can be seen separated by cell sparse IFL and IZ, respectively. (*C*) Sox2 immunostaining revealed strong labeling in the VZ/ISVZ and diffuse labeling in the IFL, OSVZ, and IZ. (*D*) Snap25 immunostaining revealed a narrow band of immunoreactive fibers bisecting the ISVZ and OSVZ extending parallel to the VZ. Diffuse Snap25 immunoreactivity is also observed in the IZ. High-power image of the fibers in IFL shown in the inset. (*E*) Immunostaining with srGAP1 revealed a similar band of fibers as seen with Snap25. The staining with srGAP1 was more diffuse and encompassed regions from IFL to IZ. CC: cortex; HC: hippocampus; ic: internal capsule; Ag: amygdala; TH: thalamus; HT: hypothalamus. Scale bars: (*A*) 1 mm, (*B–E*) 100 μm.

closer association with the germinal zone than in species without such distinctions. The concept that the ascending pathways influence rates of proliferation in the cortex and ultimately contribute to setting up distinct proliferative programs in the germinal zone and possibly determine cortical cytoarchitecture is not new (Dehay et al. 2001; Lukaszewicz et al. 2005; Carney et al. 2007). Actually, it has been demonstrated in vitro that thalamic explants can alter cell-cycle parameters in embryonic progenitor cells (Dehay et al. 2001; Dehay and Kennedy 2007) and accelerate neuronal migration in vitro (Edgar and Price 2001). However, cortical neurons are generated in roughly the same number in mouse models of "cerveau isole" (Zhou et al. 2010), indicating that this mechanism of control might have originated only in larger neocortices with a cytoarchitectonic subdivision of the germinal zones as seen in the present study. Alternatively, the IFL could accommodate fibers from newly generated projection neurons. Time-lapse recordings of newly born neurons in mouse neocortex reveal that they extend projections into the SVZ and VZ during early cortical development (Noctor et al. 2004; T Lickiss, AF Cheung, C Hutchinson, JST Taylor, Z Molnár, unpublished data). This mechanism could contribute to the regulation of neuronal production by means of such interactions.

The extent of gyrencephaly varies tremendously across species and orders. Both smooth and folded brains appear in many orders adding to the diversity in brain sizes and architecture (Cheung et al. 2007). Additionally, it has been shown that gyrencephaly is correlated to the brain weight and that the measure of gyrencephaly follows an allometric scaling specific to each order (Pillay and Manger 2007). In keeping with such studies, the appearance of convolutions during development might be due to the increased tension from white matter and other axonal fiber bundles (Van Essen 1997) or due to a thinning of the cortex (Rakic 1988; Pillay and Manger 2007) rather than simply the heterogeneous expansion of abventricular progenitors. A morphogenetic model of gyrification has been proposed that incorporates the inherent structure of the neocortex along with the elastic forces and growth of the cortex (Toro and Burnod 2005). This model uses computer simulations to suggest that convolutions are a natural consequence of cortical growth and occurs due to geometric asymmetry in the brain shape coupled with mechanical asymmetry due to differential gene expression and differential growth dynamics. In accordance with this study, it can be argued how species belonging to an otherwise gyrencephalic order violate the trend and reveal contradictory folding patterns. This might also explain why the extent of gyrencephaly varies among species.

Extending the number of species studied to date by adding agouti and marmoset, we have provided evidence of compartmentalization of the SVZ and the abundant presence of SVZ progenitor subtypes. Hence, we can conclude that these features are not related to a specific form of brain or mammalian order. On the contrary, the cortical developmental program remains relatively constant across the mammalian lineage.

While our study does not answer the mechanisms of folding itself, we provide pertinent examples to warn against generalizations based on folding or taxa. More comparative work is needed to understand why adult brains are so diverged taking into consideration variations in cortical size, folding, cell-cycle parameters, and developmental patterns.

References

Bayatti N, Sarma S, Shaw C, Eyre JA, Vouyiouklis DA, Lindsay S, Clowry GJ. 2008. Progressive loss of PAX6, TBR2, NEUROD and TBR1 mRNA gradients correlates with translocation of EMX2 to the

cortical plate during human cortical development. Eur J Neurosci. 28:1449-1456.

Carney RSE, Bystron I, López-Bendito G, Molnár Z. 2007. Comparative analysis of extra-ventricular mitoses at early stages of cortical development in rat and human. Brain Struct Funct. 212(1):37-54.

Cheung AF, Kondo S, Abdel-Mannan O, Chodroff RA, Sirey TM, Bluy LE, Webber N, DeProto J, Karlen SJ, Krubitzer L, et al. 2010. The subventricular zone is the developmental milestone of a 6-layered neocortex: comparisons in metatherian and eutherian mammals. Cereb Cortex. 20(5):1071-1081.

Cheung AF, Pollen AA, Tavare A, DeProto J, Molnár Z. 2007. Comparative aspects of cortical neurogenesis in vertebrates. J Anat. 211(2):164-176.

Collins CE, Young NA, Flaherty DK, Airey DC, Kaas JH. 2010. A rapid and reliable method of counting neurons and other cells in brain tissue: a comparison of flow cytometry and manual counting methods. Front Neuroanat. 9:4-5.

Dehay C, Kennedy H. 2007. Cell-cycle control and cortical development. Nat Rev Neurosci. 8(6):438-450.

Dehay C, Savatier P, Cortay V, Kennedy H. 2001. Cell-cycle kinetics of neocortical precursors are influenced by embryonic thalamic axons. J Neurosci. 21(1):201-214.

Edgar J, Price D. 2001. Radial migration in the cerebral cortex is enhanced by signals from the thalamus. Eur J Neurosci. 13: 1745-1754.

Fietz SA, Kelava I, Vogt J, Wilsch-Bräuninger M, Stenzel D, Fish JL, Corbeil D, Riehn A, Distler W, Nitsch R, et al. 2010. OSVZ progenitors of human and ferret neocortex are epithelial-like and expand by integrin signaling. Nat Neurosci. 13(6):690-699.

Hansen DV, Lui JH, Parker PR, Kriegstein AR. 2010. Neurogenic radial glia in the outer subventricular zone of human neocortex. Nature. 464(7288):554-561.

Haubensak W, Attardo A, Denk W, Huttner WB. 2004. Neurons arise in the basal neuroepithelium of the early mammalian telencephalon: a major site of neurogenesis. Proc Natl Acad Sci U S A. 101:3196-3201.

Hoerder-Suabedissen A, Wang WZ, Lee S, Davies KE, Goffinet AM, Rakić S, Parnavelas J, Reim K, Nicolić M, Paulsen O, et al. 2009. Novel markers reveal subpopulations of subplate neurons in the murine cerebral cortex. Cereb Cortex. 19(8):1738-1750.

Ip BK, Bayatti N, Howard NJ, Lindsay S, Clowry GJ. 2011. The corticofugal neuron-associated genes ROBO1, SRGAP1, and CTIP2 exhibit an anterior to posterior gradient of expression in early fetal human neocortex development. Cereb Cortex. 21(6):1395-1407.

Kamei Y, Inagaki N, Nishizawa M, Tsutsumi O. 1998. Visualization of mitotic radial glial lineage cells in the developing rat brain by Cdc2 kinase-phosphorylated vimentin. Glia. 23:191-199.

Kowalczyk T, Pontious A, Englund C, Daza RA, Bedogni F, Hodge R, Attardo A, Bell C, Huttner WB, Hevner RF. 2009. Intermediate neuronal progenitors (basal progenitors) produce pyramidal-projection neurons for all layers of cerebral cortex. Cereb Cortex. 19(10):2439-2450.

Lukaszewicz A, Savatier P, Cortay V, Giroud P, Huissoud C, Berland M, Kennedy H, Dehay C. 2005. G1 phase regulation, area-specific cell cycle control, and cytoarchitectonics in the primate cortex. Neuron. 47(3):353-364.

Malatesta P, Hartfuss E, Gotz M. 2000. Isolation of radial glial cells by fluorescent-activated cell sorting reveals a neuronal lineage. Development. 127:5253-5263.

Martínez-Cerdeño V, Noctor SC, Kriegstein AR. 2006. The role of intermediate progenitor cells in the evolutionary expansion of the cerebral cortex. Cereb Cortex. 16(Suppl 1):i152-i161.

Miyata T, Kawaguchi A, Saito K, Kawano M, Muto T, Ogawa M. 2004. Asymmetric production of surface-dividing and non-surface-dividing cortical progenitor cells. Development. 131(13):3133-3145.

Molnár Z. 2011. Evolution of cerebral cortical development. Brain Behav Evol. 78(1):94-107.

Molnár Z, Clowry G. 2011. Cerebral cortical development in rodents and primates. Evolution of the primate brain from neuron to behavior. Progress in brain research. Vol. 195. Oxford: Elsevier.

Neal J, Takahashi M, Silva M, Tiao G, Walsh CA, Sheen VL. 2007. Insights into the gyrification of developing ferret brain by magnetic resonance imaging. J Anat. 210(1):66-77.

Noctor SC, Flint AC, Weissman TA, Dammerman RS, Kriegstein AR. 2001. Neurons derived from radial glial cells establish radial units in neocortex. Nature. 409:714-720.

Noctor SC, Martínez-Cerdeño V, Ivic L, Kriegstein AR. 2004. Cortical neurons arise in symmetric and asymmetric division zones and migrate through specific phases. Nat Neurosci. 7(2):136-144.

Noctor SC, Martínez-Cerdeño V, Kriegstein AR. 2008. Distinct behaviors of neural stem and progenitor cells underlie cortical neurogenesis. J Comp Neurol. 508(1):28-44.

Pilaz LJ, Patti D, Marcy G, Ollier E, Pfister S, Douglas RJ, Betizeau M, Gautier E, Cortay V, Doerflinger N, et al. 2009. Forced G1-phase reduction alters mode of division, neuron number, and laminar phenotype in the cerebral cortex. Proc Natl Acad Sci U S A. 106(51):21924-21929.

Pillay P, Manger PR. 2007. Order-specific quantitative patterns of cortical gyrification. Eur J Neurosci. 25(9):2705-2712.

Pontious A, Kowalczyk T, Englund C, Hevner RF. 2008. Role of intermediate progenitor cells in cerebral cortex development. Dev Neurosci. 30(1-3):24-32.

Puzzolo E, Mallamaci A. 2010. Cortico-cerebral histogenesis in the opossum Monodelphis domestica: generation of a hexalaminar neocortex in the absence of a basal proliferative compartment. Neural Dev. 5:8.

Rakic P. 1988. Specification of cerebral cortical areas. Science. 241:170-176.

Rakic P. 1995. A small step for the cell, a giant leap for mankind: a hypothesis of neocortical expansion during evolution. Trends Neurosci. 18(9):383-388.

Rakic P. 2003. Developmental and evolutionary adaptations of cortical radial glia. Cereb Cortex. 13(6):541-549.

Reillo I, de Juan Romero C, García-Cabezas MA, Borrell V. 2011. A role for intermediate radial glia in the tangential expansion of the mammalian cerebral cortex. Cereb Cortex. 21(7):1674-1694.

Rogers J, Kochunov P, Zilles K, Shelledy W, Lancaster J, Thompson P, Duggirala R, Blangero J, Fox PT, Glahn DC, et al. 2010. On the genetic architecture of cortical folding and brain volume in primates. Neuroimage. 53(3):1103-1108.

Sessa A, Mao C, Colasante G, Nini A, Klein WH, Broccoli V. 2010. Tbr2-positive intermediate (basal) neuronal progenitors safeguard cerebral cortex expansion by controlling amplification of pallial glutamatergic neurons and attraction of subpallial GABAergic interneurons. Genes Dev. 24(16):1816-1826.

Shitamukai A, Konno D, Matsuzaki F. 2011. Oblique radial glial divisions in the developing mouse neocortex induce self-renewing progenitors outside the germinal zone that resemble primate outer subventricular zone progenitors. J Neurosci. 31(10):3683-3695.

Smart IH, Dehay C, Giroud P, Berland M, Kennedy H. 2002. Unique morphological features of the proliferative zones and postmitotic compartments of the neural epithelium giving rise to striate and extrastriate cortex in the monkey. Cereb Cortex. 12(1):37-53.

Striedter GF, Charvet CJ. 2008. Developmental origins of species differences in telencephalon and tectum size: morphometric comparisons between a parakeet (Melopsittacus undulatus) and a quail (Colinus virgianus). J Comp Neurol. 507(5):1663-1675.

Striedter GF, Charvet CJ. 2009. Telencephalon enlargement by the convergent evolution of expanded subventricular zones. Biol Lett. 5(1):134-137.

Teissier A, Griveau A, Vigier L, Piolot T, Borello U, Pierani A. 2010. A novel transient glutamatergic population migrating from the pallial-subpallial boundary contributes to neocortical development. J Neurosci. 30(31):10563-10574.

Toro R, Burnod Y. 2005. A morphogenetic model for the development of cortical convolutions. Cereb Cortex. 15(12):1900-1913.

Ulfig N, Setzer M, Neudörfer F, Bohl J. 2000. Distribution of SNAP-25 in transient neuronal circuitries of the developing human forebrain. Neuroreport. 11(6):1259-1263.

Van Essen D. 1997. A tension-based theory of morphogenesis and compact wiring in the central nervous system. Nature. 385:313-318.

Vasung L, Jovanov-Milošević N, Pletikos M, Mori S, Judaš M, Kostović I. 2011. Prominent periventricular fiber system related to ganglionic eminence and striatum in the human fetal cerebrum. Brain Struct Funct. 215(3-4):237-253.

Wang X, Tsai J, LaMonica B, Kriegstein AR. 2011. A new subtype of progenitor cell in the mouse embryonic neocortex. Nat Neurosci. 14(5):555-561.

Warner C, Goldshmit Y, Bourne JA. 2010. Retinal afferents synapse with relay cells targeting the middle temporal area in the pulvinar and lateral geniculate nuclei. Front Neuroanat. 4:8-18.

Weissman T, Noctor SC, Clinton BK, Honig LS, Kriegstein AR. 2003. Neurogenic radial glial cells in reptile, rodent and human: from mitosis to migration. Cereb Cortex. 13(6):550-559.

Zhou L, Gall D, Qu Y, Prigogine C, Cheron G, Tissir F, Schiffmann SN, Goffinet AM. 2010. Maturation of "neocortex isole" in vivo in mice. J Neurosci. 30(23):7928-7939.